AJS American Journal of Science
publishing earth-sciences research since 1818

Nesbitt, H. W., Richet, P., Henderson, G. S., & Bancroft, G. M. (2025). Partial Molar Volumes in Highly Siliceous Melts and the Relationship to Liquid Immiscibility. *American Journal of Science*, *325*, Article 8. https://doi.org/10.2475/001c.129897

Science Paper

Partial Molar Volumes in Highly Siliceous Melts and the Relationship to Liquid Immiscibility

H. Wayne Nesbitt[1][a], Pascal Richet[2], Grant S. Henderson[3], G. Michael Bancroft[4]

[1] Department of Earth Sciences, University of Western Ontario, [2] Institut de physique du globe de Paris, [3] Department of Earth Science, University of Toronto, [4] Department of Chemistry, University of Western Ontario

Keywords: partial molar volumes of components in siliceous melts, non-ideal mixing in siliceous melts, volumetric properties of siliceous melts, immiscibility in siliceous melts, cationic interactions in siliceous melts

https://doi.org/10.2475/001c.129897

American Journal of Science

Vol. 325, 2025

Partial molar volumes ($\overline{V}$) of SiO_2, K_2O, Na_2O, Li_2O and BaO have been re-evaluated in binary silicate melts at 1673 K. Volumetrically, the SiO_2 component mixes ideally in K_2O-SiO_2 melts but mixes non-ideally in Li, Na and Ba melts, with $\overline{V}_{SiO2}$ displaying maxima between ~80–95 mole% SiO_2. K_2O partial molar volumes ($\overline{V}_{K2O}$) display weak, non-ideal behaviour in K_2O-SiO_2 melts due to electrostriction, where tetrahedra collapse around the modifier cation, K^+, in response to K-O Coulombic attraction. $\overline{V}_{Na2O}$, $\overline{V}_{Li2O}$ and $\overline{V}_{BaO}$ also behave non-ideally in their respective binary melts due to electrostriction. The combined effects of non-ideal mixing of SiO_2 and electrostriction associated with the modifier cations result in molar volumes of the four melts being less than expected for ideal mixing. The extent of non-ideal volumetric mixing in the binary melts increases in the order K<Na<Li<Ba, which is the same as the order of the consolute temperatures of the miscibility gaps for these binary melts. The similar order leads us to suggest that *non-ideal volumetric mixing* results from the same chemical interactions that give rise to melt immiscibility and that these interactions are due primarily to non-ideal behaviour of the SiO_2 component.

The non-ideal volumetric mixing behaviour required use of quadratic expressions to fit molar volume-compositional trends of the four melt systems studied. Although mixing is non-ideal, the partial molar volumes of SiO_2 and modifier oxides are remarkably similar to values obtained from linear mixing models for melts containing ~45–70 wt.% SiO_2. Pronounced effects of non-ideal mixing are mostly restricted to highly siliceous melts (X_{SiO2}>0.75) where $\overline{V}_{SiO2}$ values are appreciably greater than the molar volume of liquid SiO_2 ($V°_{SiO2}$), which is ~26.75 cm^3/mole at 1673 K. The findings are consistent with volumetric (density) studies of highly siliceous (haplogranitic) melts.

1. INTRODUCTION

SiO_2 is a major component of magmas and its properties affect appreciably their densities and viscosities. Volumetric properties vary with melt composition and accurate predictive models for melt behaviour thus require accurate SiO_2 molar volumes ($V°_{SiO2}$), and partial molar volumes ($\overline{V}_{SiO2}$) of the SiO_2 component of melts over a wide range of melt compositions. An understanding of these properties also is required for industrial purposes such as production of glasses and ceramics. SiO_2 volumetric properties determine in part their response to thermal and barometric shock, thus affecting durability and reactivity. As for magmas, SiO_2 is an essential component of industrial glasses and ceramics in that many of these phases have high SiO_2 contents. There is therefore good reason to obtain highly accurate partial molar volumes of SiO_2 (and other components) in silicate melts and glasses.

The partial molar volumes of oxide components of silicate melts have been obtained successfully from density measurements by adoption of linear mixing models. (Bottinga et al., 1982, 1983; Bottinga & Weill, 1970; Courtial et al., 1999; Courtial & Dingwell, 1999, 2005, 2006; Dingwell et al., 1988; Ghiorso, 2004; Ghiorso & Kress, 2004; Lange, 1997; Lange & Carmichael, 1987, 1990; Liu & Lange, 2001, 2006). The resulting volumetric properties have been successfully applied to conditions ranging from the earth's surface to the deep mantle (Agee, 1998; Birch, 1947; Ghiorso, 2004; Ghiorso & Kress, 2004; Guillot & Sarda, 2006; Jing & Karato, 2011; Lange, 1997; Lange & Carmichael, 1987; Rigden et al., 1989; Stixrude & Karki, 2005). Experimental

a Corresponding author: hwn@uwo.ca

studies nevertheless indicate that non-linear volumetric mixing occurs in some melts for which there are numerous explanations (Bockris & Mellors, 1956; Courtial & Dingwell, 1995; Dingwell et al., 1988; Guo et al., 2013; Jackson et al., 1993; Lange & Carmichael, 1987; Nesbitt & Fleet, 1981; Shiraishi et al., 1978; Toplis, 2001). Although the linear mixing approach has been highly successful, applications generally are restricted to melts no more siliceous than about andesitic composition (SiO_2 less than ~70 mole%), in large part because many experimental studies are themselves restricted to melts of intermediate composition (~70–45 wt% SiO_2). Density studies containing greater than 70 wt.% SiO_2 are few but Knoche et al. (1995) conducted a comprehensive investigation of haplogranitic melts containing ~78 wt.% SiO_2. They reported partial molar volumes for 18 oxide components and quoted $\overline{V}_{SiO2}$ to be 27.3 cm^3/mole at 1023 K. Using their expansivity (28.18×10^{-6} K^{-1}), $\overline{V}_{SiO2}$ is 27.8 cm^3/mole at 1673 K. Nelson and Carmichael (1979), who measured melt densities containing 35–79 mole% SiO_2, obtained a $\overline{V}_{SiO2}$ value of 27.2 cm^3/mole at 1673 K, and Bourova and Richet (1998) obtained a similar value (27.3 cm^3/mole at 1670 K) by extrapolating to pure liquid SiO_2, the volume-composition trends of *silica-rich* Na_2O-SiO_2 and BaO-SiO_2 melts. Each of the last three studies focused on highly siliceous melts and the derived $\overline{V}_{SiO2}$ values were greater than those obtained by the studies of Bottinga et al. (1983), Lange and Carmichael (1987), Lange (1997) and Ghiorso and Kress (2004), who quoted respectively, 26.75, 26.90, 26.86 and 26.71 cm^3/mole for $\overline{V}_{SiO2}$. The $\overline{V}_{SiO2}$ values extracted from the various studies thus seem to correlate with the SiO_2 content of the melts studied. The differences obtained for $\overline{V}_{SiO2}$ indicate a need to understand better the interactions of components in *highly siliceous* melts and to refine the partial molar volumes of components in these melts. This study addresses the need.

1.1. Non-ideal mixing in siliceous melts

Numerous alkali and alkaline earth melts undergo phase separation (immiscibility) at highly siliceous compositions, as illustrated in figure 1 (Dietzel, 1942; Haller et al., 1974; Hess, 1996; Hudon & Baker, 2002; Kracek, 1930; A. B. Thompson et al., 2007; Veksler, 2004). The effects of non-ideal mixing are evident by the topological changes to cristobalite liquidi in Cs-, Rb-, K-, Na-, Li-, and Ba-SiO_2 melts (figs. 1A and 1B; see also fig. 2 of Veksler, 2004). The cristobalite liquidi of Cs_2O-SiO_2 and Rb_2O-SiO_2 melts are effectively the same and where composition is plotted on a logarithmic scale, the liquidi are close to linear in melts containing 0 to ~10 mole% Cs_2O or Rb_2O (Kracek, 1930, his fig. 1). From these observations Kracek (1930) noted that "The coincidence of the curves for rubidium and cesium lends itself to the interpretation that their slopes were very nearly ideal at 100% silica". On this basis he determined the enthalpy of fusion of cristobalite. Kracek (1930) also noted that the cristobalite liquidus of the K-silicate system displayed an inflection indicative of slightly non-ideal mixing. He further concluded from more pronounced inflections of the cristobalite liquidi that mixing in sodic and lithium melts was distinctly non-ideal. For alkaline earth systems, cristobalite liquidi are generally interrupted by miscibility gaps which is evidence for extreme non-ideal mixing (fig. 1B). The exception is the Ba system whose cristobalite liquidus displays an inflection so pronounced that it approaches horizontal in the region near 90 mole% SiO_2 (fig. 1B), pointing to strong non-ideal mixing in the highly siliceous portion of the system. The consolute point temperatures of the miscibility gaps of these systems increase systematically, the order being Cs~Rb<Na<Li<Ba, which is the same order of the increase in the degree of topological inflections in the cristobalite liquidi. The physical-chemical interactions leading to phase separation may also affect volumetric mixing properties in highly siliceous melts and the main objective of this study is to determine if non-ideal volumetric mixing occurs in highly siliceous melts. To this end, we quantify the degree to which non-ideal volumetric mixing occurs. Of the melts so far studied, only the densities of the K-, Na-, Li- and Ba-silicate melts have been determined in highly siliceous melts and these are the focus of the study.

2. IDEAL AND NON-IDEAL MIXING

Compositional mixing of homogeneous media may range from simple to complex with ideal volumetric mixing being the simplest. In binary systems, ideal mixing follows the relation:

$$V_{melt} = V_1^\circ X_1 + V_2^\circ X_2 \tag{1}$$

V_{melt} is the molar volume of the melt, $V°_1$ and $V°_2$ are the molar volumes of the two (pure) components '1' and '2', and X_1 and X_2 are the mole fractions of the components. Ideal mixing results in a linear trend joining the molar volumes of the pure melt components ($V°_1$ and $V°_2$) with the molar volumes of all melts of intermediate composition plotting on the linear trend. Equation (1) can be recast by substituting X_2= 1-X_1. Expanding the expression and by collecting terms, one obtains:

$$\begin{aligned} V_{melt} &= V_1^\circ X_1 + V_2^\circ (1 - X_1) \\ &= (V_1^\circ - V_2^\circ) X_1 + V_2^\circ \end{aligned} \tag{2}$$

The equation is that of a straight line of slope ($V°_1$-$V°_2$) and intercept $V°_2$. The form is convenient for fitting experimental molar volumes.

Molar volumes of non-ideal mixtures of components are more complex. Perhaps the simplest treatment of non-ideal mixing is that of the regular solution (Pitzer & Brewer, 1961, p. 282; J. B. Thompson Jr., 1967). Regular solutions mix according to a parabolic relationship (in volume versus melt composition) and they exhibit maximum deviation from ideal mixing at X_1 = X_2 = 0.50 in binary systems. The difference between the molar volume of a melt and the value calculated assuming ideal mixing is referred to as the excess molar volume of mixing (V_{ex}):

$$V_{ex} = V_{melt} - V_1^\circ X_1 - V_2^\circ X_2 \tag{3}$$

The excess molar volume of mixing for a binary, regular solution is:

$$V_{ex} = V_X X_1 X_2 \tag{4}$$

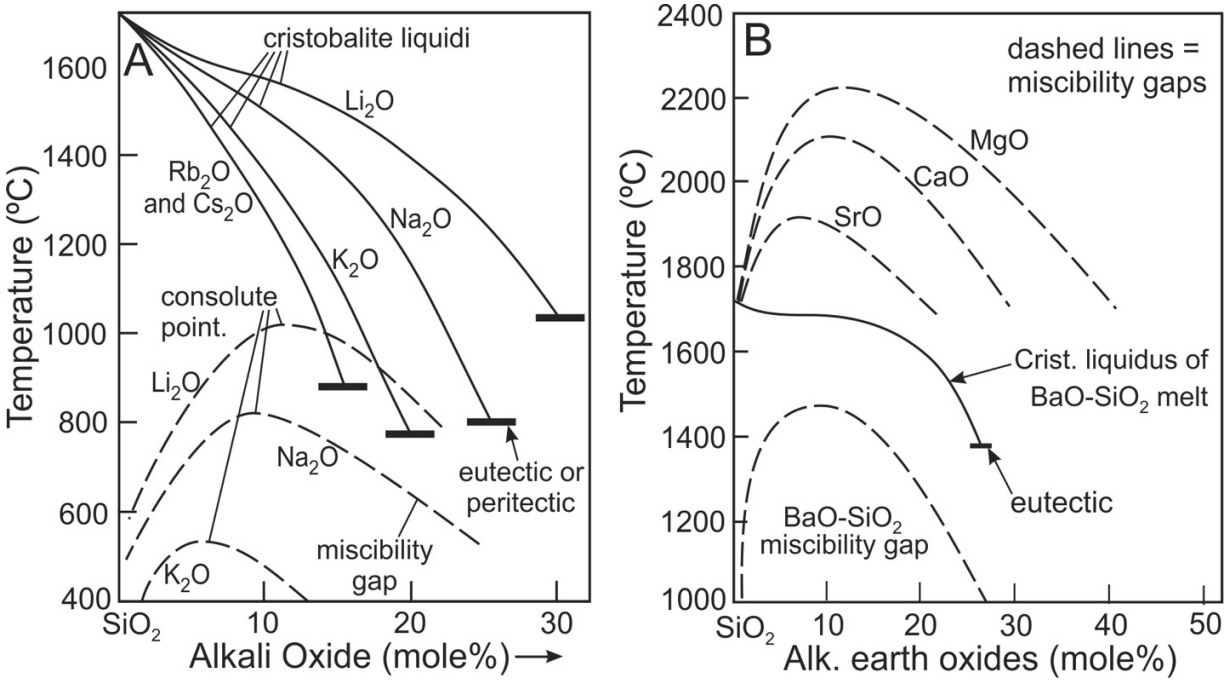

Figure 1. Portrays some cryoscopic properties of the alkali and alkaline earths silicate melts. (A) Illustrates alkali oxide-SiO_2 melt composition-temperature relationships for cristobalite liquidi (solid lines) and miscibility gaps (dashed lines) for the same systems. (B) Illustrates the cristobalite liquidus for BaO-SiO_2 melts (solid line) and the miscibility gaps for the alkaline earths-SiO_2 melt systems (dashed lines). Short, thick horizontal lines represent the termination of liquidi at either eutectic or peritectic temperatures.

where V_X is a parameter sometimes referred to as the non-ideal mixing constant (Pitzer & Brewer, 1961; J. B. Thompson Jr., 1967). The molar volumes of melts that mix regularly thus follow the relation:

$$V_{melt} = V_1^\circ X_1 + V_2^\circ X_2 + V_X X_1 X_2 \qquad (5)$$

This expression has been used previously to fit experimental melt molar volumes (Dingwell et al., 1988; Lange & Carmichael, 1987). Substitution of $X_2 = 1 - X_1$ into equation (5) yields, after expansion and collection of terms:

$$V_{melt} = A(X_1)^2 + BX_1 + C \qquad (6)$$

where

$$A = V_X;\ B = (V_1^\circ - V_2^\circ + V_X);\ C = V_2^\circ \qquad (7)$$

Equations (5) and (6) are entirely equivalent so regression of experimental melt molar volumes using either equation yields identical values for $V°_1$, $V°_2$ and V_X. The solid curve of figure 2A is the quadratic fit (eq 6) to the Ba silicate molar volume data.

3. FITS TO EXPERIMENTAL DATA

The BaO-SiO_2 melt experimental molar volumes (V_{melt}) illustrated in figure 2A describe an arcuate, concave upward trend with a minimum near 25–30 mole% BaO. The trend is poorly accounted for by a least-squares fit using the linear equation (1) (fig. 2A, dotted line), as indicated by the coefficient of determination (R^2 = 0.31). The quadratic fit using equation (6) is better (fig. 2A, solid curve, R^2 = 0.75) in that it reproduces well the arcuate trend of the data. The residuals shown in figure 2B are the differences between values obtained from the quadratic fit (V_{fit}; fig. 2A, solid curve) and the experimental melt molar volumes (V_{exptl}) with the residuals equal V_{fit}-V_{exptl}. The residuals (fig. 2B) indicate no particular bias of the quadratic fit so that the R^2 value (0.75) reflects mostly experimental uncertainty in the measurement of V_{melt}. The maximum residual value is ~0.2 cm^3/mole. Using a typical V_{melt} value of 27.0 cm^3/mole (fig. 2A), the maximum residual represents ~0.75% of melt molar volumes, thus the quadratic fit reproduces volumes within 1% of the experimental values. A similar statistical treatment of the other melt systems investigated indicates that fits to molar volumes show no bias and reproduce the experimental values to within 1%. Miscibility in the BaO-SiO_2 melt system is distinctly asymmetric (fig. 1) but there is no justification for using a volumetric mixing model more complex than a regular solution, as evident from the residuals shown in figure 2B. This does not imply, however, that volumetric mixing follows a regular solution model. Additional experimental data at greater BaO content would be required to draw such a conclusion.

The experimental data for the four melt systems shown in figure 3 were fit using equation 6 and they yield the A, B and C fit coefficients listed in table 1. The molar volumes of the two components, $V°_{SiO2}$ and $V°_{MO}$, of each system then were obtained from the A, B and C coefficients using equation (7) and these are plotted on figure 3 at the respective compositional boundaries. The dashed line joining them illustrates the ideal mixing trend for each melt system. Assuming ideal mixing, the molar volume (V_{ideal}) was calculated for each composition at which V_{melt} had been measured. V_{ideal} then was subtracted from the experimental melt volume (V_{melt}) to obtain differences ($V_{melt} - V_{ideal}$).

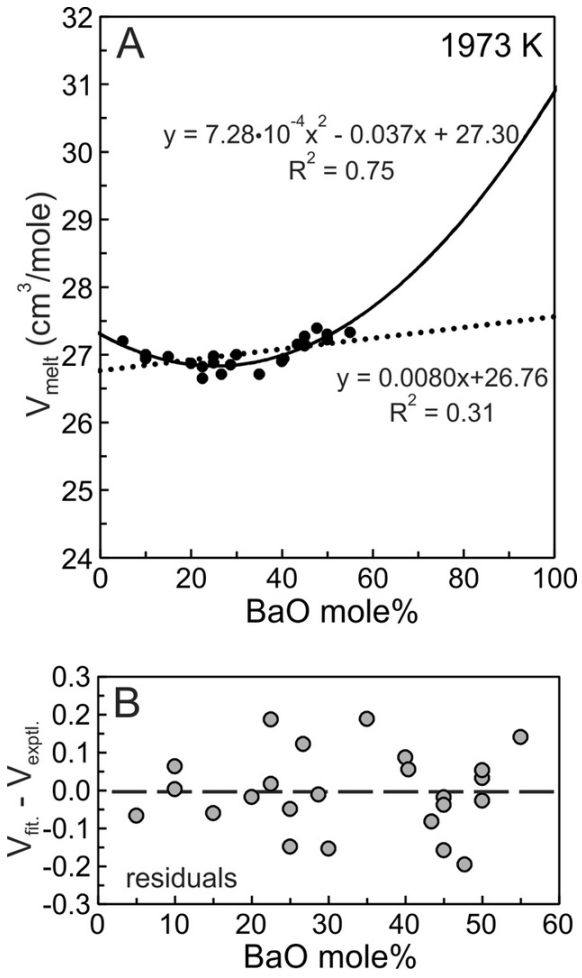

Figure 2. (A) Melt molar volumes (V_{melt}) of the BaO-SiO_2 system at 1973 K are illustrated as solid circles. The solid curve is a least squares quadratic fit to V_{melt} values and the dotted line is a linear least squares fit to the same data. The fit coefficients are provided. The 'x' and 'y' of the fit equations represent respectively 'BaO mole%' and 'V_{melt}'. R^2 is the coefficient of determination. Data are from Tomlinson et al. (1958). (B) The residuals are the differences between the quadratic fit and the experimental values plotted as shaded circles. Their random distribution about indicates that there is no substantial bias to the fit.

These are plotted on figure 4A for each system. The Ba melts display the greatest differences and from this it is concluded that they are the most non-ideal with respect to volumetric mixing. Potassic melts are closest to ideal. The conclusion is consistent with the V_X values obtained from the quadratic fits, as now emphasized. The 'A' coefficient of equation (6) (same as V_X of eq 5) is the measure of non-ideality. It decreases from 11.34×10^{-4} cm^3/mole for Ba melts to a low of 1.76×10^{-4} cm^3/mole for potassic melts (fig. 3D). Deviations from ideality decrease in the order Ba>Li>Na>K. A consequence of using a quadratic equation to fit molar volumes is that non-ideal mixing contributions are necessarily of a parabolic nature so that maximum deviation from ideality is located at 50 mole% SiO_2 (X_{SiO2} = 0.5).

4. MOLAR AND PARTIAL MOLAR VOLUMES

The partial molar volumes of SiO_2 ($\overline{V}_{SiO2}$) and modifier oxides ($\overline{V}_{MO}$) can be obtained from molar volume measurements (V_{melt}) using equations (8), (9) and (10) to solve for $\overline{V}_{SiO2}$ and $\overline{V}_{MO}$ at compositions where V_{melt} has been measured:

$$V_{melt} = \overline{V}_{SiO2} X_{SiO2} + \overline{V}_{MO} X_{MO} \qquad (8)$$

V_{melt} is the measured melt molar volume and X represents mole fraction. As shown by the dotted line in figure 3D. The slope (dy/dx) of the molar volume mixing trend at a specified composition is equal to:

$$\frac{dy}{dx} = \frac{\overline{V}_{MO} - \overline{V}_{SiO2}}{X_{MO} - X_{SiO2}} = (\overline{V}_{MO} - \overline{V}_{SiO2})/1.0 \qquad (9)$$

where X_{MO} = 1.0 and X_{SiO2} = 0.0. The slope, dy/dx, is obtained at a specified melt composition (X_{MO}) by taking the derivative of equation (6), which is:

$$\frac{dy}{dx} = 2AX_{MO} + B \qquad (10)$$

The A and B fit coefficients of equation (6) are listed in table 1 and they pertain to the MO mole% scale (see footnote 1 of table 1 to obtain 'A' and 'B' coefficients for the mole fraction scale). The values for dy/dx for each melt are provided in tables 2 to 5. The solution to the equations yields $\overline{V}_{SiO2}$ and $\overline{V}_{MO}$ and these are also listed in tables 2 to 5 at each composition for which melt molar volumes were measured.

With respect to equation (10), dy/dx may be obtained from experimental molar volumes using a finite differences approach. By this method, however, large uncertainties in the slopes may be introduced owing to uncertainties associated with individual measurements of melt densities (hence volumes) and to the choice of the compositional 'step size' used to obtain finite difference values. One avoids these uncertainties by using the slope (dy/dx) of the best fit quadratic equation (6), where dy/dx is evaluated at compositions for which V_{melt} has been measured.

4.1. Molar volume of SiO_2 ($V°_{SiO2}$)

Although liquid SiO_2 has a specific $V°_{SiO2}$ value at 1673 K and 101.3 kPa, the quadratic fits to molar volumes shown in figure 3 yield $V°_{SiO2}$ values of 26.75, 27.13, 27.30, and 27.58 cm^3/mole respectively for the K, Na, Li and Ba systems. These values follow the order of the non-ideal mixing term, V_X, of figure 4A, the implication being that non-ideal mixing affects at least some of the *retrieved* $V°_{SiO2}$ values. Because the K-silicate melts are closest to ideal (fig. 4A) this system should yield the best estimate of $V°_{SiO2}$, which is 26.75 cm^3/mole. The value is adopted for 1673 K and it is similar to those reported by the comprehensive studies of Bottinga et al. (1983), Lange and Carmichael (1987), Lange (1997) and Ghiorso and Kress (2004). Their values were 26.75, 26.90, 26.86, and 26.71cm^3/mole respectively. We emphasize, however, that our adopted $V°_{SiO2}$ value (26.75 cm^3/mole) has been determined for a system displaying minor non-deal mixing.

A somewhat more accurate value may be obtained from Cs and Rb melts in that they seem to mix effectively ideally (Kracek, 1930). Sasek and Lisy (1972a, 1972b) reported the

Table 1. Fit parameters and volumetric constants for alkali and Ba silicate melts

Melt	Constants for Equation 6			Constants of Equation 5			Constants of eq. 13	
	A^1	B^1	C^1	$V°_{MO}{}^{1,2}$	$V°_{SiO2}{}^{1,2}$	$V_X{}^1$	m^1	b^1
Free quadratic least-squares fit coefficients and V° values								
Li_2O-SiO_2[3]	4.00×10^{-4}	-12.7×10^{-2}	27.30	18.60	27.30	4.00×10^{-4}	0.076	-12.1
Na_2O-SiO_2[3]	2.94×10^{-4}	0.024×10^{-2}	27.13	30.09	27.13	2.94×10^{-4}	0.0625	-15.55
K_2O-SiO_2[3]	1.76×10^{-4}	18.89×10^{-2}	26.75	47.40	26.75	1.76×10^{-4}	0.0424	-16.06
BaO-SiO_2[3]	11.34×10^{-4}	-7.60×10^{-2}	27.58	31.32	27.58	11.3×10^{-4}	0.2605	-80.9
Linear least-squares fit coefficients and $V°$ values with $V°_{SiO2}$ = 26.75 cm^3/mole								
Li_2O-SiO_2[3]	9.45×10^{-5}	-9.98×10^{-2}	26.75	17.72	26.75	9.45×10^{-5}		
Na_2O-SiO_2[3]	2.35×10^{-5}	2.16×10^{-2}	26.75	29.15	26.75	2.35×10^{-5}		
K_2O-SiO_2[3]	1.76×10^{-4}	1.89×10^{-1}	26.75	47.40	26.75	1.76×10^{-4}		
Li_2O-SiO_2[4]	0	-0.0933	26.75	17.42	26.75	0		
Na_2O-SiO_2[4]	0	0.023	26.75	29.05	26.75	0		
Rb_2O-SiO_2[4]	0	0.2697	26.75	53.72	26.75	0		
Cs_2O-SiO_2[4]	0	0.4056	26.75	67.31	26.75	0		

1 - Units are cm^3/mole. Constants are for mole% scale. Constants for the mole fraction scale are obtained by multiplying 'A' by 10^4 and multiplying 'B' by 10^2. There is no change to C.
2 - MO = component 1; SiO_2 = component 2
3 - Bockris and Mellors (1956)
4 - Sasek and Lisy (1972a, 1972b)

densities of Li-, Na-, Rb- and Cs-silicate melts at 1673 K (fig. 4B). There are too few data to employ meaningful quadratic fits to the Rb and Cs systems so that linear, least-squares fits were employed with $V°_{SiO2}$ fixed at 26.75 cm^3/mole. The fits (fig. 4B) and the fit coefficients ($V°_{M2O}$) are listed in table 1. Nascimento (2007) compiled measurements on Rb and Cs silicate glasses containing ~1–60 mole% alkali oxide. For both systems experimental glass molar volume trends between ~1–10 mole% describe slightly arcuate trends, implying minor non-ideal mixing in the highly siliceous glasses (Nascimento, 2007, see his fig. 2). Additional density measurements on Rb_2O-SiO_2 and Cs_2O-SiO_2 melt systems are wanted at highly siliceous concentrations to obtain a more robust value for $V°_{SiO2}$.

4.2. Partial molar volumes ($\overline{V}_{SiO2}$ and $\overline{V}_{MO}$)

The partial molar volumes of SiO_2 and modifier oxides (MO) derived from the fits (fig. 3) using equations (8) to (10) are listed in tables 2 to 5 and are plotted on figure 5 where the solid lines emphasize the trends. The horizontal dashed lines emanating from $V°_{SiO2}$ on each diagram (fig. 5) indicate $\overline{V}_{SiO2}$ values that would result if mixing were ideal. In potassic melts containing up to ~45 mole% K_2O (fig. 5A), $\overline{V}_{SiO2}$ is effectively the same as $V°_{SiO2}$ thus $\overline{V}_{SiO2}$ behaves ideally (within experimental uncertainty). The situation is different for $\overline{V}_{K2O}$. If it were to mix ideally, $\overline{V}_{K2O}$ would follow the horizontal dashed line emanating from $V°_{K2O}$ (fig. 5A). Instead it increases somewhat in progressively more potassic melts. It is the K_2O component that gives rise to non-ideal mixing in this system. It accounts for the V_X value of 1.76×10^{-4} cm^3/mole (fig. 4A) and to the slight curvature of V_{melt} in figure 3C. The non-ideal behaviour of K_2O results from collapse of tetrahedra around the cation (Nesbitt et al., 2022), as addressed in the next section.

$\overline{V}_{SiO2}$ values of the Li, Na and Ba melts are not constant and instead achieve maxima between about 95 and 80 mole% SiO_2 (fig. 5B, 5C, 5D). After achieving a maximum value, $\overline{V}_{SiO2}$ decreases with progressive increase in modifier oxide content for each system. $\overline{V}_{SiO2}$ mixes non-ideally in Li, Na and Ba melts. Relative to $V°_{SiO2}$ (26.75 cm^3/mole), the maxima in $\overline{V}_{SiO2}$ become more pronounced in the order K<Na<Li<Ba, which is consistent with the progressive increase in V_X (fig. 4A), with the consolute temperatures (fig. 1), and with the extent to which the topology of the cristobalite liquidi deviate from linearity in figure 1. $\overline{V}_{Na2O}$, $\overline{V}_{Li2O}$ and $\overline{V}_{BaO}$ values increase with MO content (fig. 5), thus both SiO_2 and MO behave non-ideally in Na_2O-SiO_2, Li_2O-SiO_2 and BaO-SiO_2 melts.

5. ELECTROSTRICTION

The partial molar volumes of all modifier oxides are affected by electrostriction (Nesbitt et al., 2022). It results from a reaction between O atoms of Si tetrahedra and modifier cations whereby Coulombic attraction causes tetrahedra to collapse around cations (Marcus, 2011; Nesbitt et al., 2022; Pitzer & Brewer, 1961, pp. 500–502) thereby decreasing melt molar volumes and altering modifier oxide and SiO_2 partial molar volumes. The extent of collapse depends on the charge and size of the modifier cation; the greater its charge the stronger the force of attraction and the greater the extent of collapse around the cation. Also, the greater the size of the cation the greater the number of SiO_4 tetrahedra that can collapse around the cation. The reaction results in non-ideal mixing of all modifier oxide

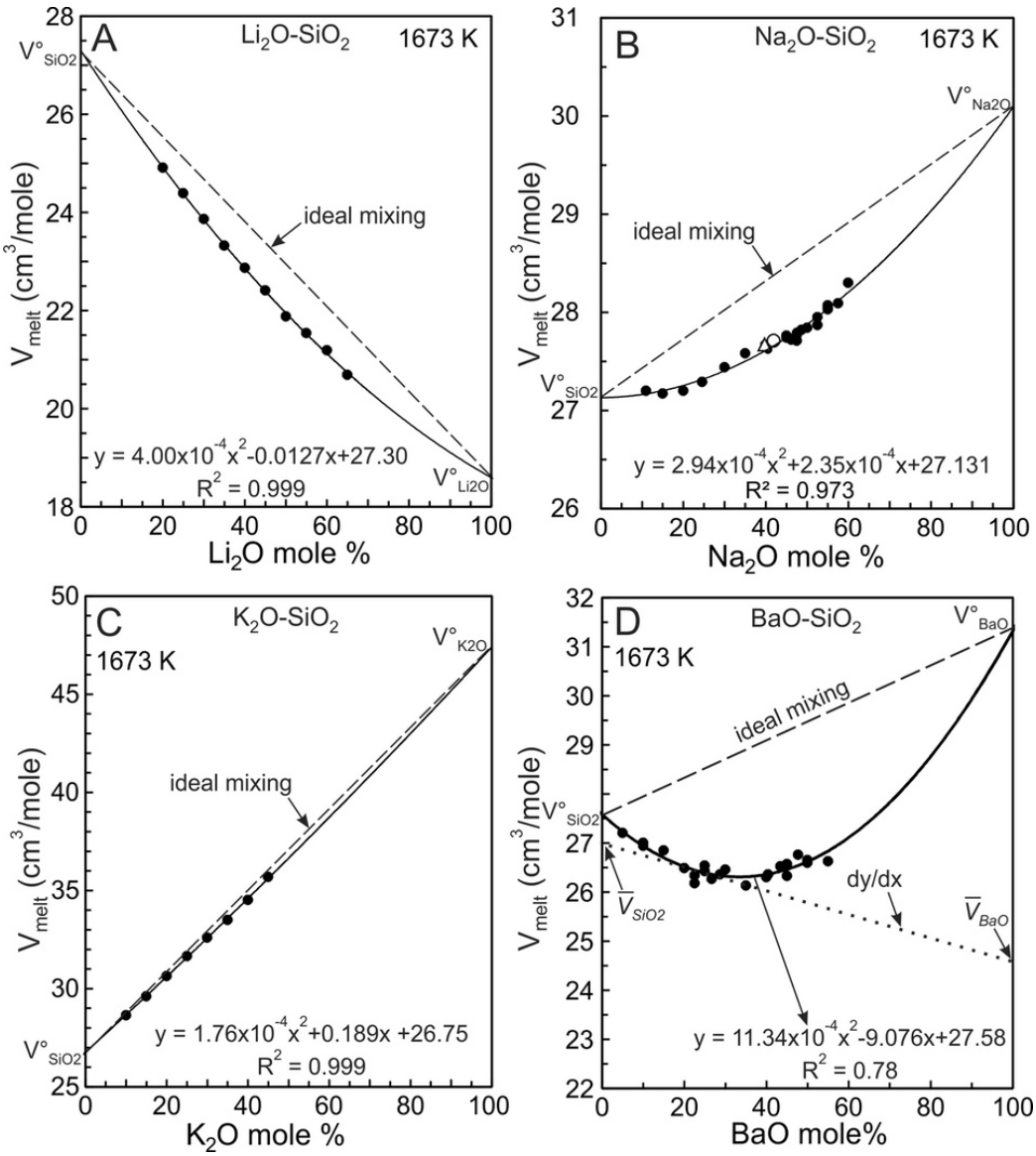

Figure 3. Molar volumes of Li_2O-SiO_2, Na_2O-SiO_2, K_2O-SiO_2 and BaO-SiO_2 melts. The solid circles are experimental results of Bockris et al. (1956). The molar volumes of BaO-SiO_2 melts have been calculated at 1673 K using expansivities of Tomlinson et al. (1958). See figure 2A for the experimental data at 1973 K. The open symbols of figure 3B are experimental points of Stein et al. (1986) and Dingwell et al. (1988). The solid lines are quadratic best fits to the experimental data and the dashed lines are ideal mixing curves using the molar volumes of the respective components ($V°_{SiO2}$ and $V°_{MO}$) obtained from the quadratic fits. The 'x' and 'y' values of the fit equations represent modifier oxide mole% and V_{melt} respectively. The dotted line of figure 3D is the slope of the molar volume trend taken at 22 mole% BaO.

components in silicate melts. Electrostriction also accounts for: (1) establishment of the oxygen coordination polyhedra of cations; (2) consistent cation coordination numbers (CNs) and; (3) establishment of equilibrium M-O bond distances in melts. Where the Coulombic force of attraction is sufficiently strong, SiO_4 tetrahedra beyond the first coordination sphere may collapse toward the cation (Nesbitt et al., 2022). The electronegativity of the cation may also contribute to collapse in that the M-O bond is unlikely to be entirely ionic. The greater the covalent character of the bond the stronger should be the bond and the shorter should be the bond distance, which should affect collapse.

Following Nesbitt et al. (2022), $\overline{V}_{MO}$ is composed of two terms. One is the volume occupied by the polyhedral cage (V_{Poly}) surrounding the modifier cation. The other relates to the extent of volume collapse of tetrahedra around the cation (V_{Col}):

$$\overline{V}_{MO} = V_{Poly} + V_{Col} \quad (11)$$

From Nesbitt et al. (2022), V_{Poly} is given by:

$$V_{Poly} = \left(\frac{4\pi}{3}\right) d^3 + 6.83\ (\text{Å}^3\ per\ atom) \quad (12)$$

where 'd' is equilibrium M-O bond distance, which is the sum of the ionic radii of the modifier cation and O^{2-} derived from crystalline silicates (Huheey et al., 1993; Navrotsky et al., 1985). The constant (6.83 Å^3/atom) is an 'excluded

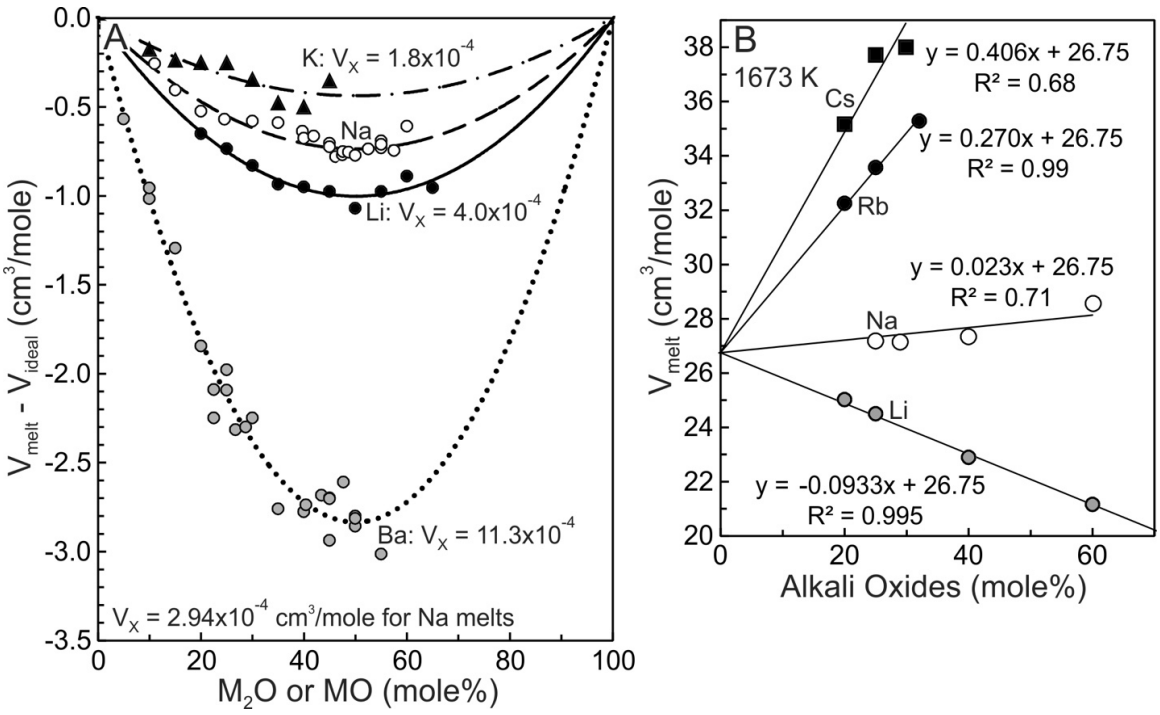

Figure 4. (A) Difference between experimental melt molar volumes (V_{melt}) and the volume of the melt (at the same composition) assuming mixing were ideal. The differences are plotted as a function of melt composition. The non-ideal mixing constant, V_X, for the Li, K and Ba melt systems are quoted. The V_X value for the Na system is provided at the bottom of the diagram (to retain clarity). (B) Symbols represent experimental melt molar volumes of Cs, Rb, Na and Li silicate melts measured by Sasek and Lisy (1972a, 1972b). The lines represent linear least squares fits to the data. The 'x' and 'y' values of the fit equations represent modifier oxide mole% and V_{melt} respectively.

Table 2. Molar, partial molar volumes and V_{Col} for K_2O-SiO_2 melts at 1673 K.

K_2O	$V°_{melt}$ exptl.	$V°_{melt}$ fit	derivative[1] of fit eqn.	$\overline{V}_{SiO2}$	$\overline{V}_{K2O}$	$\overline{V}_{K2O}$	V_{Col}[2]
mole%	cm^3/mole	cm^3/mole	(*dy/dx*)	cm^3/mole	cm^3/mole	Å^3/atom	Å^3/atom
0.0		26.75	0.1889	26.75			
10.0	28.64	28.66	0.1924	26.72	45.96	76.34	-15.72
15.0	29.61	29.62	0.1942	26.70	46.12	76.60	-15.46
20.0	30.63	30.60	0.1959	26.71	46.31	76.92	-15.14
25.0	31.66	31.58	0.1977	26.72	46.49	77.22	-14.84
30.0	32.60	32.58	0.1995	26.62	46.56	77.35	-14.71
35.0	33.50	33.58	0.2012	26.46	46.58	77.38	-14.68
40.0	34.51	34.59	0.2030	26.39	46.69	77.56	-14.50
45.0	35.69	35.61	0.2048	26.48	46.95	77.99	-14.07
100.0		47.40	0.2241	24.99[3]	47.40[3]	78.74	-13.32

1 - Fit equation: $Ax^2 + Bx + C$: $dy/dx = 2Ax + B$; x = mole% of modifier oxide
2 - V_{Col} equals V_{Poly} - $\overline{V}_{K2O}$ where V_{Poly} = 97.99 Å^3/atom. See text for details.
3 - Equation (5) and coefficients of table 1 were used to calculate these values.

volume' common to all alkali and alkaline earths modifier cations. The V_{Poly} term is independent of melt composition and is 37.41, 61.19, 92.06 and 115.46 Å^3/atom respectively for Li, Na, K and Ba. Following Nesbitt et al. (2022), V_{Col} values for the Li, Na, K and Ba silicate melts were calculated using equation (11) by subtracting the appropriate V_{Poly} from $\overline{V}_{MO}$ of tables 2–5. V_{Col} values for Mg, Ca, and Sr melts were similarly calculated after evaluating $\overline{V}_{MO}$ at 1673 K using the expansivities of Tomlinson et al. (1958). All V_{Col} values are plotted on figure 6. In each system, V_{Col} increases effectively linearly with increasing modifier oxide content:

Table 3. Molar and partial molar volumes, and V_{Col} of Na_2O-SiO_2 melts at 1673 K.

Na_2O	$V°_{melt}$ exptl.	$V°_{melt}$ fit	derivative[1] of fit eqn.	$\overline{V}_{SiO2}$	$\overline{V}_{Na2O}$	$\overline{V}_{Na2O}$	V_{Col}[2]
mole%	cm^3/mole	cm^3/mole	(*dy/dx*)	cm^3/mole	cm^3/mole	Å^3/atom	Å^3/atom
0.0		27.13	0.0002	26.75			
11.0	27.20	27.17	0.0067	27.13	27.80	46.17	-15.02
15.0	27.17	27.20	0.0091	27.03	27.94	46.41	-14.78
20.0	27.20	27.25	0.0120	26.96	28.16	46.78	-14.41
24.6	27.29	27.31	0.0147	26.93	28.40	47.17	-14.02
30.0	27.44	27.40	0.0179	26.90	28.69	47.66	-13.53
35.0	27.58	27.50	0.0208	26.85	28.93	48.06	-13.13
39.7	27.67	27.60	0.0236	26.73	29.09	48.33	-12.86
40.0	27.64	27.61	0.0238	26.69	29.07	48.28	-12.91
41.9	27.71	27.66	0.0249	26.67	29.16	48.43	-12.76
45.0	27.76	27.74	0.0267	26.56	29.23	48.55	-12.64
45.0	27.74	27.74	0.0267	26.54	29.21	48.52	-12.67
46.2	27.72	27.77	0.0274	26.45	29.19	48.50	-12.69
47.5	27.71	27.81	0.0282	26.37	29.19	48.49	-12.70
47.5	27.77	27.81	0.0282	26.43	29.25	48.59	-12.60
47.6	27.79	27.81	0.0282	26.45	29.27	48.62	-12.57
48.7	27.82	27.84	0.0289	26.41	29.30	48.67	-12.52
50.0	27.84	27.88	0.0296	26.36	29.32	48.71	-12.48
52.5	27.87	27.95	0.0311	26.24	29.35	48.75	-12.44
52.5	27.95	27.95	0.0311	26.32	29.43	48.88	-12.31
55.0	28.07	28.03	0.0326	26.28	29.54	49.06	-12.13
55.0	28.03	28.03	0.0326	26.24	29.50	49.00	-12.19
55.0	28.05	28.03	0.0326	26.26	29.52	49.03	-12.16
57.5	28.09	28.12	0.0340	26.13	29.54	49.06	-12.13
60.0	28.30	28.20	0.0355	26.17	29.72	49.37	-11.82
100.0		30.09	0.0590	24.19[3]	30.09[3]	49.99	-11.20

1 - Fit equation: $Ax^2 + Bx + C$: $dy/dx = 2Ax + B$; x = mole% of modifier oxide
2 - V_{Col} equals V_{Poly}- $\overline{V}_{Na2O}$ where V_{Poly} = 54.36 Å^3/atom. See text for details.
3 - Equation (5) and coefficients of table 1 were used to calculate these values.

$$V_{Col} = m\,(M_{MO}) + b \qquad (13)$$

where '*m*' is the slope, '*b*' is the intercept and M_{MO} is mole% of MO (modifier oxide). The data were fit using a linear least-squares approach and the resulting '*m*' and '*b*' fit coefficients are included in table 1 for Li, Na, K and Ba melts. Fit coefficients for Mg, Ca and Sr melts are provided in figure 6. The value of '*b*' represents V_{Col} at 100 mole% SiO_2, which is the value of V_{Col} *at infinite dilution of the modifier oxide*. Substituting the appropriate V_{Col} value into equation (11) gives $\overline{V}_{MO}$ at *infinite dilution*. Inspection of the slopes of the trends for Li, Na, K and Ba silicate melts indicate that they do not change appreciably in highly siliceous melts so that the estimates of $\overline{V}_{MO}$ at infinite dilution seem robust.

The V_{Col} values for Rb_2O and Cs_2O are not plotted on figure 6 for lack of experimental melt molar volumes as a function of composition. Bottinga et al. (1983) nevertheless obtained $\overline{V}_{Rb2O}$ and $\overline{V}_{Cs2O}$ from the data available (fig. 4), and V_{Col} values were determined to be -27.6 and -25.5 cm^3/mole respectively (Nesbitt et al., 2022). These melts thus mix non-ideally due to electrostriction but the effect of non-ideal mixing is likely to be minimal, as for the K_2O-SiO_2 system (fig. 3C). The SiO_2 component of Rb and Cs melts likely behaves ideally, as in K_2O melts (fig. 5A). Additional measurements of densities of highly siliceous binary melt systems are required to evaluate better the partial molar volumes of the components of these systems.

6. MELT MOLAR VOLUME TRENDS

$\overline{V}_{SiO2}$ behaviour is close to ideal in K silicate melts (fig. 5A) whereas $\overline{V}_{K2O}$ behaves somewhat non-ideally due to electrostriction. With collapse of tetrahedra toward the cation, the melt volume (V_{melt}) decreases to a value less than expected for ideal mixing (fig. 3C). $\overline{V}_{K2O}$ has its lowest value at infinite dilution (fig. 6A), thus the effect of electrostriction has its greatest effect, *per mole of K_2O*, in the most siliceous melts. Because $\overline{V}_{K2O}$ increases somewhat with in-

Table 4. Molar, partial molar volumes and V_{Col} for Li_2O-SiO_2 melts at 1673 K.

Li_2O	$V°_{melt}$ exptl.	$V°_{melt}$ fit	derivative[1] of fit eqn.	$\overline{V}_{SiO2}$	$\overline{V}_{Li2O}$	$\overline{V}_{Li2O}$	V_{Col}[2]
mole%	cm^3/mole	cm^3/mole	(*dy/dx*)	cm^3/mole	cm^3/mole	Å^3/atom	Å^3/atom
0		27.30	-0.1150	26.75	(~14.6)		
20.00	24.91	24.92	-0.1110	27.13	16.03	26.63	-10.78
25.00	24.39	24.38	-0.1070	27.07	16.37	27.18	-10.23
30.00	23.86	23.85	-0.1030	26.95	16.65	27.66	-9.75
35.00	23.32	23.35	-0.0990	26.79	16.89	28.05	-9.36
40.00	22.87	22.86	-0.0950	26.67	17.17	28.52	-8.89
45.00	22.41	22.40	-0.0910	26.51	17.41	28.91	-8.50
50.00	21.88	21.95	-0.0870	26.23	17.53	29.12	-8.29
55.00	21.54	21.53	-0.0830	26.11	17.81	29.58	-7.83
60.00	21.19	21.12	-0.0790	25.93	18.03	29.95	-7.46
65.00	20.69	20.74	-0.0750	25.57	18.07	30.01	-7.40
100.00		18.60	-0.0710	23.30[3]	18.60[3]	30.90	-6.51

1 - Fit equation: $Ax^2 + Bx + C$: $dy/dx = 2Ax + B$; x = mole% of modifier oxide
2 - V_{Col} equals V_{Poly}- $\overline{V}_{Li2O}$ where V_{Poly}= 30.58 Å^3/atom. See text for details.
3 - Equation (5) and coefficients of table 1 were used to calculate these values.

creased K_2O content of the melt (fig. 5A) a weak concave upward V_{melt} trend is observed (fig. 3C, solid curve). To summarize, with collapse of tetrahedra around K^+, and with $\overline{V}_{SiO2}$ effectively constant (fig. 5A), the melts display molar volumes slightly less than expected for ideal mixing. Electrostriction is responsible for the weak non-ideal behaviour.

The dashed lines of figure 6 illustrate that $\overline{V}_{K2O}$, $\overline{V}_{Na2O}$, $\overline{V}_{Li2O}$ and $\overline{V}_{BaO}$ have their lowest values at infinite dilution (X_{SiO2} = 1.0) and all increase with modifier oxide content of the melt. The four binary systems display qualitatively similar mixing trends (fig. 3) in that all are weakly to strongly concave upward. The enhanced concavity of the Na, Li and Ba melts results both from the large $\overline{V}_{SiO2}$ values at compositions between ~95 and ~80 mole% SiO_2 (figs. 5B, 5C, 5D), and from the continuous increase in $\overline{V}_{MO}$ with modifier oxide content of the melts. Concavity of the melts becomes greater in the order K< Na<Li<Ba, which is the order of V_X values (fig. 4A). Both components, SiO_2 and MO, contribute to non-ideal mixing in Na, Li and Ba silicate melts whereas only the K_2O component makes a contribution in the potassic melts.

6.1. Gibbs-Duhem test for thermodynamic consistency

The partial molar volume trends illustrated in fig. 5 are constrained to obey the Gibbs-Duhem equation, one form of which is (Rowlinson, 1969, p. 125):

$$X_{SiO2}\left(\frac{\partial \overline{V}_{SiO2}}{\partial X_{SiO2}}\right)_{P,T} = X_{MO}\left(\frac{\partial \overline{V}_{MO}}{\partial X_{MO}}\right)_{P,T} \qquad (14)$$

There is a maximum in $\overline{V}_{SiO2}$ in the Ba, Li and Na silicate melts (Fig. 5) and $\partial \overline{V}_{SiO2}/\partial X_{SiO2}$ at each maximum is 0.0. Because X_{SiO2} and X_{MO} are non-zero at these maxima, $\partial \overline{V}_{MO}/\partial X_{MO}$ must be 0.0 (a minimum) for equation (14) to be satisfied. It is a thermodynamic necessity. This behaviour is observed in other liquid systems, as discussed and illustrated by Rowlinson (1969, p. 125). Experimental results for the Ba, Li and Na silicate melt systems unfortunately do not extend to sufficiently large X_{SiO2} values to provide experimental evidence for minima in $\partial \overline{V}_{MO}/\partial X_{MO}$. Additional experimental studies of highly siliceous melts are wanted. With such studies a more fundamental understanding of the physical chemical behaviour of these melts will be obtained.

7. DISCUSSION

7.1. Reactions and non-ideal mixing

The electrostriction reaction contributes to non-ideal mixing in all melts containing modifier oxides. Its maximum effect occurs at infinite dilution of the modifier oxide and as apparent from figure 6, the order of $\overline{V}_{MO}$ *at infinite dilution* is Li<Na<K<Mg<Ca<Sr<Ba. The order is different from the order of V_X values (fig. 4A) and we conclude that electrostriction is not the major contributor to the non-ideal volumetric mixing in Na, Li or Ba melts. According to Kracek (1930) the SiO_2 component of Cs and Rb melts mix ideally or nearly so. Assuming V_X is effectively zero for these melts, the degree of non-ideal mixing, based on V_X values (fig. 4A), increases in the order Cs=Rb<K<Na<Li<Ba. Consolute point temperatures follow the same order (fig. 1; see also Hess, 1996). Also, consolute point compositions typically are located at ~90 mole% SiO_2 (fig. 1; Haller et al., 1974; Hess, 1996). $\overline{V}_{SiO2}$ values for Na, Li and Ba melts display maxima in the same compositional range (fig. 5) so that cryoscopic observations (fig. 1), the V_X values (fig. 4A) and the maxima in $\overline{V}_{SiO2}$ (fig. 5) all indicate that non-ideal volumetric mixing increases in the order

Table 5. Molar and partial molar volumes, and V_{Col} of BaO-SiO_2 melts at 1673 K.

BaO	$V°_{melt}$ exptl.	$V°_{melt}$ fit	derivative[1] of fit eqn.	$\overline{V}_{SiO2}$	$\overline{V}_{BaO}$	$\overline{V}_{BaO}$	V_{Col}[2]
mole%	cm^3/mole	cm^3/mole	(*dy/dx*)	cm^3/mole	cm^3/mole	Å^3/atom	Å^3/atom
0		27.58	-0.0760	26.75			
5.00	27.20	27.23	-0.0646	27.52	21.06	34.98	-80.48
10.00	26.94	26.93	-0.0533	27.47	22.14	36.78	-78.68
10.00	27.00	26.93	-0.0533	27.53	22.20	36.88	-78.58
15.00	26.85	26.70	-0.0419	27.48	23.28	38.68	-76.78
20.00	26.49	26.52	-0.0306	27.10	24.04	39.93	-75.53
22.50	26.17	26.45	-0.0249	26.74	24.24	40.27	-75.19
22.50	26.33	26.45	-0.0249	26.89	24.40	40.53	-74.93
25.00	26.54	26.39	-0.0193	27.02	25.09	41.68	-73.78
25.00	26.42	26.39	-0.0193	26.91	24.98	41.49	-73.97
26.70	26.27	26.36	-0.0154	26.68	25.14	41.75	-73.71
28.70	26.36	26.33	-0.0109	26.67	25.58	42.49	-72.97
30.00	26.45	26.32	-0.0079	26.69	25.90	43.02	-72.44
35.00	26.13	26.31	0.0034	26.01	26.35	43.78	-71.68
40.00	26.30	26.36	0.0148	25.71	27.19	45.16	-70.30
40.40	26.36	26.36	0.0157	25.72	27.29	45.33	-70.13
43.40	26.52	26.42	0.0225	25.55	27.79	46.17	-69.29
45.00	26.57	26.46	0.0261	25.39	28.00	46.52	-68.94
45.00	26.33	26.46	0.0261	25.15	27.76	46.12	-69.34
45.00	26.56	26.46	0.0261	25.39	28.00	46.51	-68.95
47.70	26.76	26.54	0.0322	25.22	28.44	47.24	-68.22
50.00	26.65	26.62	0.0374	24.78	28.52	47.38	-68.08
50.00	26.59	26.62	0.0374	24.72	28.47	47.29	-68.17
50.00	26.64	26.62	0.0374	24.77	28.51	47.36	-68.10
55.00	26.63	26.83	0.0488	23.94	28.82	47.87	-67.59
100.00		31.32	0.1508	16.24[3]	31.32[3]	52.03	-63.43

1 - Fit equation: $Ax^2 + Bx + C$: $dy/dx = 2Ax + B$; x = mole% of modifier oxide
2 - V_{Col} equals V_{Poly}- $\overline{V}_{BaO}$. V_{Poly} = 93.94 Å^3/atom. See text for details.
3 - Equation (5) and coefficients of table 1 were used to calculate these values.

Cs~Rb<K<Na<Li<Ba. From these observations, we suggest that the physical-chemical interactions giving rise to phase separation in alkali and alkaline earths silicate melts also affect the volumetric properties of these melts, with the contributions to non-ideal volumetric mixing increasing in the order K<Na<Li<Ba. The minor non-ideal volumetric mixing in Cs, Rb and K melts likely arises mostly from electrostriction, with V_X for Cs and Rb melts likely being less than the value obtained for K silicate melts (fig. 4A)

7.2. Phase separation and $\overline{V}_{SiO2}$

Hess (1996, his fig. 9) noted a remarkably strong correlation between consolute point temperatures and the 'ionic potential' of alkali and alkaline earths modifier cations. Hudon and Baker (2002) extended the relationship to include other cations. Hess (1996) argued that immiscibility observed in highly siliceous melts resulted from repulsive interactions of modifier cations (M-M) due primarily to insufficient 'shielding' of modifier cations by BOs, which dominate highly siliceous melts. In melts of greater modifier oxide content immiscibility does not occur because NBOs provide better shielding from M-M interactions than BOs. A premise of the hypothesis is that dissolution of alkali oxides in SiO_2-rich melt results in modifier cations remaining in close proximity after dissolution. Subsequent studies make the 'close proximity' argument uncertain, although they do not disprove it. Above ~600–700 K, sodic glasses are fast ion conductors with Na^+ being highly mobile (Lei et al., 2015). It should be still more mobile in melts. Also, above ~700 K, ^{23}Na static NMR experiments indicate that Na motion is rapid enough to average out Na-Na dipolar couplings and that Na^+ acts in a liquid-like manner at and above ~900 K (George et al., 1998). Modifier cations thus may be well dispersed in melts. In support of the Hess hypothesis we add a role for Si, where both Si-M *and* M-M repulsive interactions contribute to and are responsible for phase separation. As for M-M repulsion, Si-M repulsion

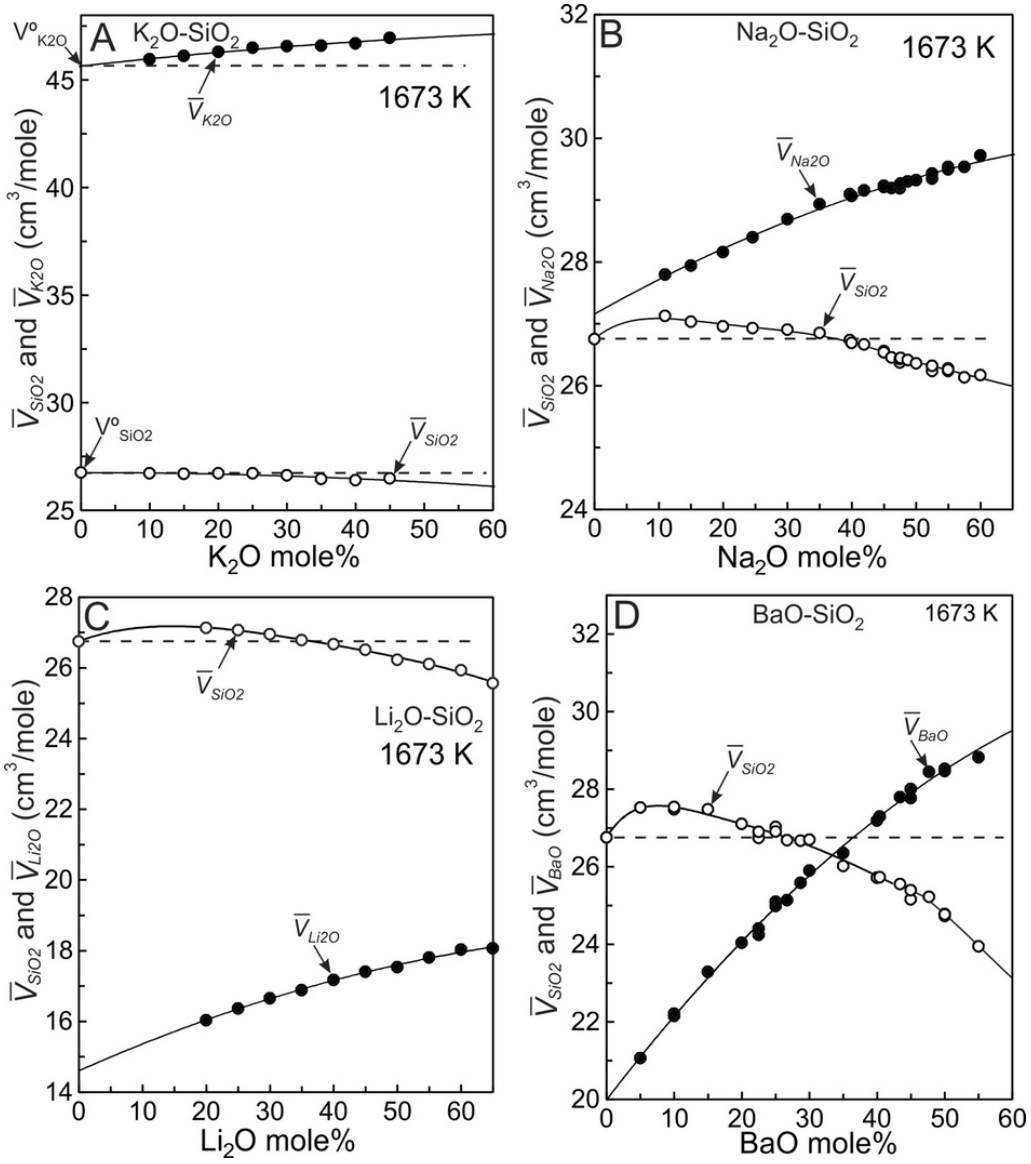

Figure 5. Partial molar volumes of the components of the binary alkali and Ba silicate melts. The solid curves are drawn to emphasize the trends of the partial molar volumes as a function of composition. They are not best fits. The dashed straight lines represent values of $\overline{V}_{SiO2}$ (and $\overline{V}_{K2O}$) if the component were to mix ideally.

should give rise to a strong correlation between consolute point temperatures and the 'ionic potential' of the modifier cations as emphasized by Hess (1996). We now elaborate on Si-M interactions.

The first coordination sphere of a modifier cation is composed of oxygen atoms (both NBO and BO) which, in turn, are bonded to Si atoms so that ~3–8 Si atoms should be present in the second coordination spheres of alkali and alkaline earth cations (Du & Cormack, 2004; Du & Corrales, 2006, their table 6; Micoulaut, 2008; Navrotsky et al., 1985). Si-M Coulombic repulsion thus is expected. Consider a Na^+ to be coordinated to three O atoms on the face of a Si tetrahedron (fig. 7A) where all Na-O bond distances are 2.35Å, all Si-O bond distances are 1.61Å (Huheey et al., 1993) and all O-Si-O angles to be 109.47° (tetrahedral angle). The distance separating Si and Na then is ~2.33Å, as proven by solution of triangles SiOC, OCD and SiCD to obtain Si-D = 0.536Å (fig. 7A). An equivalent solution to triangle NaCD, with Na-O = 2.35Å yields a D-Na distance of 1.794Å and the sum of Si-D + D-Na is the Si-Na distance and equal to 2.33Å. The Si-Na bond distance is similar to the O-Na bond distance (2.35Å). Considering that Si has a greater positive partial charge than NBO and BO have negative partial charges (Demiralp et al., 1999; Hsieh et al., 1994), Si-Na repulsion should be appreciable. In another arrangement where Na is bonded to two O atoms of a tetrahedron (an edge), the solution to the triangles yields a *maximum* Si-Na separation of 2.88Å as shown in figure 7B where Na, Si and the two O atoms are located on the plane drawn. Si-Na repulsion again should be appreciable. The above calculations may be repeated with other alkali ions. Si-Li repulsion should be stronger than Si-Na repulsion at equilibrium bond distances due to the smaller size of Li. Si-K repulsion should be weaker. Si-modifier cation repulsion thus is likely to contribute to phase separation much as M-M repulsion does.

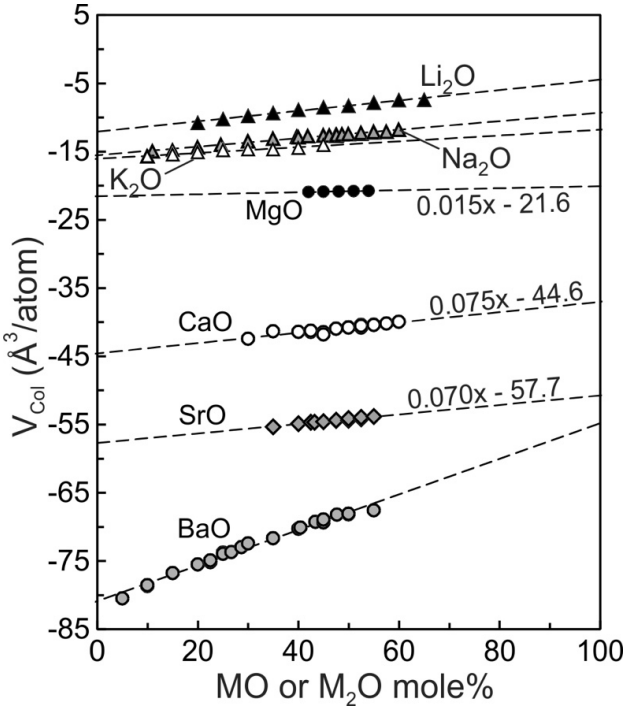

Figure 6. Volume collapse (V_{Col}) as a function of melt composition for numerous alkali and alkaline earth silicate melts. Volume collapse, which results from electrostriction, has been calculated with equations (10) and (11). The dashed lines represent linear least squares fits to the seven sets of data.

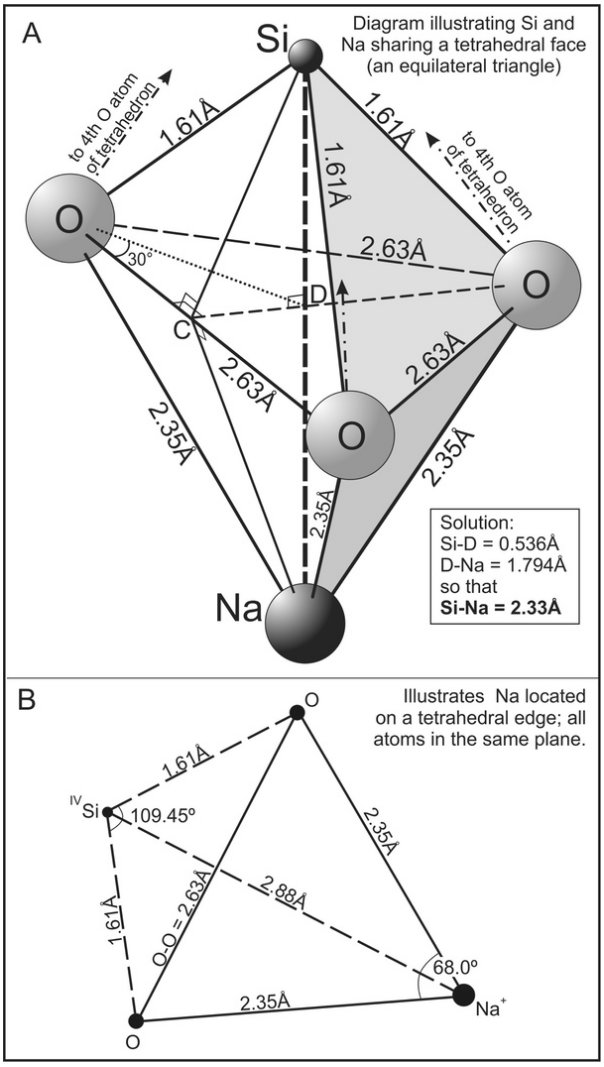

Figure 7. The face of a SiO_4 tetrahedron (three O atoms) is shared by both a Si and a Na^+. Equilibrium Si-O and Na-O bond distances (1.61Å and 2.35Å respectively) are employed and the O-Si-O angle is taken as 109.45°. With these values the distance separating Si and Na^+ is 2.33Å, which is slightly shorter than the Na-O equilibrium bond distance (2.35Å). Strong repulsion must occur, making it unlikely that Na^+ is bonded to three O atoms of any one tetrahedron in glasses and melts.

The magnitude of the repulsive (and attractive) forces depends on the partial charges on the modifier cation (M), Si, BO and NBO of the tetrahedra. Hsieh et al. (1994) determined partial charges on atoms of $Na_2Si_2O_5$ glass using X-ray photoelectron spectroscopic (XPS) studies and differences in partial charges of NBO and BO were confirmed experimentally by Nesbitt et al. (2017). For Q^4 species, Hsieh et al. (1994) obtained partial charges on Si and BO of +1.27 and -0.63 respectively, which are similar to the MD simulations of Demiralp et al. (1999), who obtained Si and BO partial charges of +1.32 and -0.66 on Q^4 species. Hsieh et al. (1994) also determined partial charges on Si, BO, NBO and Na of Q^3 species to be +1.23, -0.64, -0.96 and +0.68 respectively. Hess (1996) emphasized that NBO 'shields' M^+ from other M^+ better than BO. NBO also shields M^+ from Si better than BO. In highly siliceous melts where BO greatly dominates, phase separation may result from the combined effect of M-M and Si-M repulsion. The Hess hypothesis may also explain the greater $\overline{V}_{SiO2}$ values in ~90 mole% SiO_2 melts than $V°_{SiO2}$ of v-SiO_2 (fig. 5B to 5D). Si-M and M-M repulsion may be responsible. Determination of densities of Cs, Rb, K, Na, Li and Ba melts containing between ~100–80 mole% SiO_2 are required to understand better $\overline{V}_{SiO2}$ and $\overline{V}_{MO}$ values in highly siliceous melts.

Thermodynamic treatments of immiscibility have been performed but these provide little insight into the physical-chemical interactions at the atomic-molecular level (e.g., Kim & Sanders, 1999 and references therein). Simulations may provide insight into the above-noted interactions but we offer a note of caution. Both attractive and repulsive interactions are dependent on the partial charges of the atoms involved. If these interactions are to be properly investigated, the partial charges (electron density) on the atoms should be determined from first principles molecular orbital calculations. Assignment of partial charges to atoms prior to molecular dynamics calculations (e.g., Du & Corrales, 2006, their table 2) may not be appropriate in that both experiments and simulations indicate that partial charges vary depending on local environments (Demiralp et al., 1999; Hsieh et al., 1994). The appropriate calculations should provide substantial insight into the both volume collapse and the Hess hypothesis.

7.3. Partial molar volumes compared with previous results

Many previous studies used linear equations to extract partial molar volumes of the oxide components (Bottinga et al., 1982, 1983; Bottinga & Weill, 1970; Ghiorso & Kress, 2004; Lange, 1997; Lange & Carmichael, 1987, 1990). These studies made clear that the extracted partial molar volumes applied to restricted compositional ranges, typically ~45–70 mole% SiO_2. Within this compositional range, partial molar volumes obtained using linear equations are remarkably similar to values obtained here using the quadratic equation (6) to fit melt molar volumes. Bottinga et al. (1983), and Ghiorso and Kress (2004) obtained $\overline{V}_{SiO2}$ = 26.75 and 26.71 cm^3/mole respectively. Our approach yields 26.75 cm^3/mole. With respect to modifier oxides, our $\overline{V}_{Na2O}$ values of melts containing ~45 to ~65 mole% SiO_2 range between ~28.9 and ~29.5 cm^3/mole (fig. 5B). The $\overline{V}_{Na2O}$ value quoted by Ghiorso and Kress (2004) is 29.1 cm^3/mole. Bottinga et al. (1983) obtained 29.03 cm^3/mole. The major differences between $\overline{V}_{SiO2}$ and $\overline{V}_{MO}$ values obtained here, and with linear mixing models, become apparent in *highly siliceous* melts ($SiO_2 \geq 75$ mole%). Our results are in accord with those of Knoche et al. (1995) who determined partial molar volumes of components in haplogranitic melts. Their experimental value for $\overline{V}_{SiO2}$ is ~27.8 cm^3/mol at 1673 K, indicating that $\overline{V}_{SiO2}$ is greater in haplogranitic melts than in andesitic to basaltic melts. This analysis indicates that the maximum values of $\overline{V}_{SiO2}$ in Na, Li and Ba melts range between ~27.1 to ~27.5 cm^3/mole and that the maxima are achieved at compositions between ~80 and 95 mole% SiO_2 (fig. 5). Melts studied by Knoche et al. (1995) contained 12.5 mole% Al_2O_3 and its effects on $\overline{V}_{SiO2}$ and other components are unknown. Nevertheless, non-ideal mixing of SiO_2 in *highly siliceous melts* helps to rationalize experimental results spanning a compositional range from ~100 to ~45 mole% SiO_2.

8. CONCLUSIONS

Two non-ideal volumetric mixing contributions have been identified in alkali and alkaline earths binary silicate melts. The partial molar volumes of modifier oxides ($\overline{V}_{MO}$) behave non-ideally due to electrostriction. The Coulombic force of attraction between modifier cation and O atoms of Si tetrahedra causes the tetrahedra to collapse toward modifier cations. The reaction decreases the molar volumes of melts and of $\overline{V}_{MO}$. A contribution to non-ideal mixing may arise from the SiO_2 component. SiO_2 mixes ideally in siliceous potassic melts and it probably mixes similarly in siliceous Rb and Cs melts. In melts containing Na, Li and Ba, however, SiO_2 mixes non-ideally and $\overline{V}_{SiO2}$ displays maxima between ~95 and 80 mole% SiO_2. The extent to which SiO_2 deviates from ideal mixing correlates strongly with the topological properties of cristobalite liquidi and with consolute point temperatures of the respective alkali and alkaline earth silicate melts. We propose that a common reaction is responsible for phase separation, for topological differences in the cristobalite liquidi, and for the non-ideal volumetric mixing behaviour of SiO_2 in the highly siliceous melts. The reaction may involve Si-M and M-M repulsive interactions but their nature and strength remain problematic.

ACKNOWLEDGMENTS

HWN thanks Dr. K. Harrison for many discussions concerning calculations of Coulombic interactions among Si, O and modifier cations. The discussions made much clearer the complexities of Si-O-M interactions. We also thank Drs. Bernard de Jong for reading a draft of the manuscript and offering insightful comments. Two reviewers, including Dr. Kai Hess, provided highly insightful reviews which resulted in substantial improvement to the manuscript. GSH acknowledges funding in the form of a NSERC discovery grant. We thank the editors, Drs. M. Brandon (editor) and E. Moulas (Assoc. editor) for their input to the manuscript, and our respective departments and universities for the logistical support required to conduct this study.

AUTHOR CONTRIBUTIONS

All authors contributed to the ideas included in the ms. It is impossible to assign to individual authors the various conceptual contributions because a concept expressed by one inevitably has been altered and expanded by another. The majority of the writing was performed by HWN and PR, although all contributed to the writing and editing of the ms.

Editor: Mark Brandon, Associate Editor: Evangelos Moulas

Submitted: September 05, 2023 EDT. Accepted: February 17, 2025 EDT. Published: April 04, 2025 EDT.

REFERENCES

Agee, C. B. (1998). Crystal–liquid density inversions in terrestrial and lunar magmas. *Physics of the Earth and Planetary Interiors*, *107*(1–3), 63–74. https://doi.org/10.1016/s0031-9201(97)00124-6

Birch, F. (1947). Finite elastic strain of cubic crystals. *Physical Review*, *71*(11), 809–824. https://doi.org/10.1103/physrev.71.809

Bockris, J. O. M., & Mellors, G. W. (1956). Electric Transport in Liquid Lead Silicates and Borates. *The Journal of Physical Chemistry*, *60*(9), 1321–1328. https://doi.org/10.1021/j150543a040

Bockris, J. O. M., Tomlinson, J. W., & White, J. L. (1956). The structure of the liquid silicates: partial molar volumes and expansivities. *Transactions of the Faraday Society*, *52*, 299–310. https://doi.org/10.1039/tf9565200299

Bottinga, Y., Richet, P., & Weill, D. F. (1983). Calculation of the density and thermal expansion coefficient of silicate liquids. *Bulletin de Minéralogie*, *106*(1), 129–138. https://doi.org/10.3406/bulmi.1983.7675

Bottinga, Y., & Weill, D. F. (1970). Densities of liquid silicate systems calculated from partial molar volumes of oxide components. *American Journal of Science*, *269*(2), 169–182. https://doi.org/10.2475/ajs.269.2.169

Bottinga, Y., Weill, D., & Richet, P. (1982). Density calculations for silicate liquids. I. Revised method for aluminosilicate compositions. *Geochimica et Cosmochimica Acta*, *46*(6), 909–919. https://doi.org/10.1016/0016-7037(82)90047-3

Bourova, E., & Richet, P. (1998). Quartz and cristobalite: high-temperature cell parameters and volumes of fusion. *Geophysical Research Letters*, *25*(13), 2333–2336. https://doi.org/10.1029/98gl01581

Courtial, P., & Dingwell, D. B. (1995). Nonlinear composition dependence of molar volume of melts in the CaO-Al_2O_3-SiO_2 system. *Geochimica et Cosmochimica Acta*, *59*(18), 3685–3695. https://doi.org/10.1016/0016-7037(95)00272-2

Courtial, P., & Dingwell, D. B. (1999). Densities of melts in the CaO-MgO-Al_2O_3-SiO_2 system. *American Mineralogist*, *84*(4), 465–476. https://doi.org/10.2138/am-1999-0401

Courtial, P., & Dingwell, D. B. (2005). High-temperature density of lanthanide-bearing Na-silicate melts: Partial molar volumes for Ce_2O_3, Pr_2O_3, Nd_2O_3, Sm_2O_3, Eu_2O_3, Gd_2O_3, Tb_2O_3, Dy_2O_3, Ho_2O_3, Er_2O_3, Tm_2O_3, and Yb_2O_3. *American Mineralogist*, *90*(10), 1597–1605. https://doi.org/10.2138/am.2005.1786

Courtial, P., & Dingwell, D. B. (2006). A partial molar volume for La_2O_3 in silicate melts. *Journal of Non-Crystalline Solids*, *352*, 304–314. https://doi.org/10.1016/j.jnoncrysol.2005.12.002

Courtial, P., Gottsmann, J., Holzheid, A., & Dingwell, D. B. (1999). Partial molar volumes of NiO and CoO liquids: implications for the pressure dependence of metal-silicate partitioning. *Earth and Planetary Science Letters*, *171*(1), 171–183. https://doi.org/10.1016/s0012-821x(99)00142-9

Demiralp, E., Çağin, T., & Goddard, W. A. (1999). Morse Stretch Potential Charge Equilibrium Force Field for Ceramics: Application to the Quartz-Stishovite Phase Transition and to Silica Glass. *Physical Review Letters*, *82*(8), 1708–1711. https://doi.org/10.1103/physrevlett.82.1708

Dietzel, A. (1942). The cation field strengths and their relation to devitrifying processes, to compound formation and to the melting points of silicates. *Zeitschrift fuer Elektrochemie und Angewandte Physikalische Chemie*, *48*, 9–23. https://doi.org/10.1002/bbpc.19420480104

Dingwell, D. B., Brearley, M., & Dickinson, J. E., Jr. (1988). Melt densities in the Na_2O-FeO-Fe_2O_3-SiO_2 system and the partial molar volume of tetrahedrally-coordinated ferric iron in silicate melts. *Geochimica et Cosmochimica Acta*, *52*(10), 2467–2475. https://doi.org/10.1016/0016-7037(88)90305-5

Du, J., & Cormack, A. N. (2004). The medium range structure of sodium silicate glasses: a molecular dynamics simulation. *Journal of Non-Crystalline Solids*, *349*, 66–79. https://doi.org/10.1016/j.jnoncrysol.2004.08.264

Du, J., & Corrales, L. R. (2006). Compositional dependence of the first sharp diffraction peaks in alkali silicate glasses: A molecular dynamics study. *Journal of Non-Crystalline Solids*, *352*(30–31), 3255–3269. https://doi.org/10.1016/j.jnoncrysol.2006.05.025

George, A. M., Richet, P., & Stebbins, J. F. (1998). Cation dynamics and premelting in lithium metasilicate (Li_2SiO_3) and sodium metasilicate (Na_2SiO_3); a high-temperature NMR study. *American Mineralogist*, *83*(11-12 Part 1), 1277–1284. https://doi.org/10.2138/am-1998-11-1216

Ghiorso, M. S. (2004). An equation of state for silicate melts. I. Formulation of a general model. *American Journal of Science*, *304*(8–9), 637–678. https://doi.org/10.2475/ajs.304.8-9.637

Ghiorso, M. S., & Kress, V. C. (2004). An equation of state for silicate melts. II. Calibration of volumetric properties at 105 Pa. *American Journal of Science*, *304*(8–9), 679–751. https://doi.org/10.2475/ajs.304.8-9.679

Guillot, B., & Sarda, P. (2006). The effect of compression on noble gas solubility in silicate melts and consequences for degassing at mid-ocean ridges. *Geochimica et Cosmochimica Acta*, *70*(5), 1215–1230. https://doi.org/10.1016/j.gca.2005.11.007

Guo, X., Lange, R. A., & Ai, Y. (2013). The density and compressibility of CaO-FeO-SiO_2 liquids at one bar: Evidence for four-coordinated Fe^{2+} in the $CaFeO_2$ component. *Geochimica et Cosmochimica Acta*, *120*, 206–219. https://doi.org/10.1016/j.gca.2013.06.007

Haller, W., Blackburn, D. H., & Simmons, J. H. (1974). Miscibility gaps in alkali-silicate binaries—data and thermodynamic interpretation. *Journal of the American Ceramics Society*, *57*, 120–126. https://doi.org/10.1111/j.1151-2916.1974.tb10832.x

Hess, P. C. (1996). Upper and lower critical points: Thermodynamic constraints on the solution properties of silicate melts. *Geochimica et Cosmochimica Acta*, *60*(13), 2365–2377. https://doi.org/10.1016/0016-7037(96)00095-6

Hsieh, C. H., Jain, H., Miller, A. C., & Kamitsos, E. I. (1994). X-ray photoelectron spectroscopy of Al- and B-substituted sodium trisilicate glasses. *Journal of Non-Crystalline Solids*, *168*(3), 247–257. https://doi.org/10.1016/0022-3093(94)90336-0

Hudon, P., & Baker, D. R. (2002). The nature of phase separation in binary oxide melts and glasses. I. Silicate systems. *Journal of Non-Crystalline Solids*, *303*(3), 299–345. https://doi.org/10.1016/s0022-3093(02)01043-8

Huheey, J. E., Keiter, E. A., & Keiter, R. L. (1993). *Inorganic Chemistry: Principles of Structure and Reactivity* (4th ed.). HarperCollins College Publishers.

Jackson, W. E., Mustre de Leon, J., Brown, G. E., Jr., Waychunas, G. A., Conradson, S. D., & Combes, J.-M. (1993). High-Temperature XAS Study of Fe_2SiO_4 Liquid: Reduced Coordination of Ferrous Iron. *Science*, *262*(5131), 229–233. https://doi.org/10.1126/science.262.5131.229

Jing, Z., & Karato, S. I. (2011). A new approach to the equation of state of silicate melts: An application of the theory of hard sphere mixtures. *Geochimica et Cosmochimica Acta*, *75*(22), 6780–6802. https://doi.org/10.1016/j.gca.2011.09.004

Kim, S. S., & Sanders, T. H. (1999). Thermodynamic Modeling of the Miscibility Gaps and the Metastable Liquidi in the MgO-SiO_2, CaO-SiO_2, and SrO-SiO_2 Systems. *Journal of the American Ceramic Society*, *82*(7), 1901–1907. https://doi.org/10.1111/j.1151-2916.1999.tb02014.x

Knoche, R., Dingwell, D. B., & Webb, S. L. (1995). Melt densities for leucogranites and granitic pegmatites: Partial molar volumes for SiO_2, Al_2O_3, Na_2O, K_2O, Li_2O, Rb_2O, Cs_2O, MgO, CaO, SrO, BaO, B_2O_3, P_2O_5, F_2O_{-1}, TiO_2, Nb_2O_5, Ta_2O_5, and WO_3. *Geochimica et Cosmochimica Acta*, *59*(22), 4645–4652. https://doi.org/10.1016/0016-7037(95)00328-2

Kracek, F. C. (1930). The cristobalite liquidus in the alkali oxide-silica systems and the heat of fusion of cristobalite. *Journal of Physical Chemistry*, *52*(4), 1436–1442. https://doi.org/10.1021/ja01367a021

Lange, R. A. (1997). A revised model for the density and thermal expansivity of K_2O-Na_2O-CaO-MgO-Al_2O_3-SiO_2 liquids from 700 to 1900 K: extension to crustal magmatic temperatures. *Contributions to Mineralogy and Petrology*, *130*(1), 1–11. https://doi.org/10.1007/s004100050345

Lange, R. A., & Carmichael, I. S. E. (1987). Densities of Na_2O-K_2O-CaO-MgO-FeO-Fe_2O_3-$A_{12}O_3$-TiO_2-SiO_2 liquids: New measurements and derived partial molar properties. *Geochimica et Cosmochimica Acta*, *51*(11), 2931–2946. https://doi.org/10.1016/0016-7037(87)90368-1

Lange, R. A., & Carmichael, I. S. E. (1990). Thermodynamic properties of silicate liquids with emphasis on density, thermal expansion and compressibility. In *Modern methods of igneous petrology* (pp. 25–64). https://doi.org/10.1515/9781501508769-006

Lei, X., Jee, Y., & Huang, K. (2015). Amorphous $Na_2Si_2O_5$ as a fast Na+ conductor: an ab initio molecular dynamics simulation. *Journal of Materials Chemistry A*, *3*(39), 19920–19927. https://doi.org/10.1039/c5ta04474j

Liu, Q., & Lange, R. A. (2001). The partial molar volume and thermal expansivity of TiO_2 in alkali silicate melts: Systematic variation with Ti coordination. *Geochimica et Cosmochimica Acta*, *65*(14), 2379–2393. https://doi.org/10.1016/s0016-7037(01)00565-8

Liu, Q., & Lange, R. A. (2006). The partial molar volume of Fe_2O_3 in alkali silicate melts: Evidence for an average Fe^{3+} coordination number near five. *American Mineralogist*, *91*(2–3), 385–393. https://doi.org/10.2138/am.2006.1902

Marcus, Y. (2011). Electrostriction in electrolyte solutions. *Chemical Reviews*, *111*(4), 2761–2783. https://doi.org/10.1021/cr100130d

Micoulaut, M. (2008). Amorphous materials: Properties, structure, and durability: Constrained interactions, rigidity, adaptative networks, and their role for the description of silicates. *American Mineralogist*, *93*(11–12), 1732–1748. https://doi.org/10.2138/am.2008.2903

Nascimento, M. L. F. (2007). Correlation between Conductivity and Free Volume in Rubidium and Cesium Silicate Glasses. *Brazilian Journal of Physics*, *37*(2a), 429–434. https://doi.org/10.1590/s0103-97332007000300014

Navrotsky, A., Geisinger, K. L., McMillan, P., & Gibbs, G. V. (1985). The tetrahedral framework in glasses and melts-inferences from molecular orbital calculations and implications for structure, thermodynamics and Physical Properties. *Physics and Chemistry of Minerals*, *11*(6), 284–298. https://doi.org/10.1007/bf00307406

Nelson, S. A., & Carmichael, I. S. E. (1979). Partial molar volumes of oxide components in silicate liquids. *Contributions to Mineralogy and Petrology*, *71*(2), 117–124. https://doi.org/10.1007/bf00375427

Nesbitt, H. W., & Fleet, M. E. (1981). An ion-association model for PbO-SiO_2 melts: interpretation of thermochemical, conductivity, and density data. *Geochimica et Cosmochimica Acta*, *45*(2), 235–244. https://doi.org/10.1016/0016-7037(81)90168-x

Nesbitt, H. W., Henderson, G. S., Bancroft, G. M., & O'Shaughnessy, C. (2017). Electron densities over Si and O atoms of tetrahedra and their impact on Raman stretching frequencies and Si-NBO force constants. *Chemical Geology*, *461*, 65–74. https://doi.org/10.1016/j.chemgeo.2016.11.022

Nesbitt, H. W., Richet, P., Bancroft, G. M., & Henderson, G. S. (2022). Partial molar volumes of metal oxides in silicate melts: effects of coulombic interactions. *American Journal of Science*, *322*(5), 683–704. https://doi.org/10.2475/05.2022.02

Pitzer, K. S., & Brewer, L. (1961). *Thermodynamics* (2nd ed.). McGraw-Hill Book Co.

Rigden, S. M., Ahrens, T. J., & Stolper, E. M. (1989). High pressure equation of state of molten anorthite and diopside. *Journal of Geophysical Research: Solid Earth*, *94*(B7), 9508–9522. https://doi.org/10.1029/jb094ib07p09508

Rowlinson, J. S. (1969). *Liquids and liquid mixtures* (2nd ed.). Butterworths & Co.

Sasek, L., & Lisy, A. (1972a). Structure and properties of silicate melts I. *Sbornik Vysoke Skoly Chemlcko-Technologicke, Silikatu*, *L2*, 165–215.

Sasek, L., & Lisy, A. (1972b). Structure and properties of silicate melts II. *Sbornik Vysoke Skoly Chemlcko-Technologicke, Silikatu*, *L2*, 217–254.

Shiraishi, Y., Ikeda, K., Tamura, A., & Saitô, T. (1978). On the viscosity and density of the molten FeO-SiO_2 system. *Transactions, Journal of International Metallurgy*, *19*(5), 264–274. https://doi.org/10.2320/matertrans1960.19.264

Stein, D. J., Stebbins, J. F., & Carmichael, I. S. E. (1986). Density of molten sodium aluminosilicates. *Journal of the American Ceramics Society*, *69*(5), 396–399. https://doi.org/10.1111/j.1151-2916.1986.tb04767.x

Stixrude, L., & Karki, B. (2005). Structure and freezing of $MgSiO_3$ liquid in the Earth's lower mantle. *Science*, *310*, 297–299. https://doi.org/10.1126/science.1116952

Thompson, A. B., Aerts, M., & Hack, A. C. (2007). Liquid immiscibility in silicate melts and related systems. *Reviews in Mineralogy and Geochemistry*, *65*(1), 99–127. https://doi.org/10.2138/rmg.2007.65.4

Thompson, J. B., Jr. (1967). Thermodynamic Properties of Simple Solutions. In P. H. Abelson (Ed.), *Researches in geochemistry* (Vol. 2, pp. 340–361). J. Wiley & Sons Inc.

Tomlinson, J. W., Heynes, M. S. R., & Bockris, J. O. M. (1958). The structure of liquid silicates part 2.–molar volumes and expansivities. *Transactions of the Faraday Society*, *54*, 1822–1833. https://doi.org/10.1039/tf9585401822

Toplis, M. J. (2001). Quantitative links between microscopic properties and viscosity of liquids in the system SiO_2-Na_2O. *Chemical Geology*, *174*, 321–331. https://doi.org/10.1016/s0009-2541(00)00323-5

Veksler, I. V. (2004). Liquid immiscibility and its role at the magmatic-hydrothermal transition: a summary of experimental studies. *Chemical Geology*, *210*(1–4), 7–31. https://doi.org/10.1016/j.chemgeo.2004.06.002